Stem Cell Reports
Article

ISSCR

OPEN ACCESS

Neuroblast migration along cellular substrates in the developing porcine brain

Demisha D.L. Porter,[1,2] Sara N. Henry,[2] Sadia Ahmed,[2] Amy L. Rizzo,[4] Rita Makhlouf,[3] Collin Gregg,[1] and Paul D. Morton[2,*]

[1]Virginia Tech Graduate Program in Translational Biology, Medicine and Health, Virginia Polytechnic Institute and State University, Roanoke, VA, USA
[2]Department of Biological Sciences and Pathobiology, Virginia-Maryland College of Veterinary Medicine, Virginia Polytechnic Institute and State University, Blacksburg, VA, USA
[3]Department of Biological Sciences, Virginia Polytechnic Institute and State University, Blacksburg, VA, USA
[4]Office of the University Veterinarian & Animal Resources, Virginia Polytechnic Institute and State University, Blacksburg, VA, USA
*Correspondence: pmorton@vt.edu
https://doi.org/10.1016/j.stemcr.2022.07.015

SUMMARY

In the past decade it has become evident that neuroblasts continue to supply the human cortex with interneurons via unique migratory streams shortly following birth. Owing to the size of the human brain, these newborn neurons must migrate long distances through complex cellular landscapes to reach their final locations. This process is poorly understood, largely because of technical difficulties in acquiring and studying neurotypical postmortem human samples along with diverging developmental features of well-studied mouse models. We reasoned that migratory streams of neuroblasts utilize cellular substrates, such as blood vessels, to guide their trek from the subventricular zone to distant cortical targets. Here, we evaluate the association between young interneuronal migratory streams and their preferred cellular substrates in gyrencephalic piglets during the developmental equivalent of human birth, infancy, and toddlerhood.

INTRODUCTION

The mammalian cortex varies in size and organization across species. Neocortical expansion has benefited from a continuous production of neurons following birth (Alvarez-Buylla and Garcia-Verdugo, 2002; Azevedo et al., 2009; Lois and Alvarez-Buylla, 1994; Luskin, 1993; Walton, 2012). During early postnatal periods of development, the subventricular zone (SVZ), housing the largest pool of neural stem/progenitor cells (NSPCs), promotes cortical expansion (Sanai et al., 2005). NSPCs give rise to immature neurons (neuroblasts) that migrate to their final destinations in various regions of the human brain, including the ventromedial prefrontal cortex (vPFC) and the anterior cingulate cortex (Aoyagi et al., 2018; Lazarini and Lledo, 2011; Lois et al., 1996; Paredes et al., 2016a; Sanai et al., 2011; Sawamoto et al., 2011). The journey from site of origin to final destination is largely influenced by the size and complexity of the brain, as neuroblasts must migrate significantly further through dense cellular networks in larger brains.

To supply the brain in such a manner requiring long migratory treks, it has been speculated that neuroblasts utilize cellular substrates for guidance. Two main cellular substrates have been proposed to facilitate migration, namely glial cells (gliophilic) and blood vessels (vasophilic). Following birth, elongated chains of migrating neuroblasts are tightly packed within glial tubes, encased by astrocytic processes, in the mammalian subventricular zone/rostral migratory stem (SVZ/RMS) core (Gengatharan et al., 2016; Kornack and Rakic, 2001; Lois et al., 1996; Peretto et al., 2005). Impairments to the organization of glial tubes in postnatal and adult mice were associated with chain migration defects to the olfactory bulb (OB), suggesting that neuroblast-astrocyte interactions are essential for this mode of transport (Anton et al., 2004; Belvindrah et al., 2007; Chazal et al., 2000; Kaneko et al., 2010).

The vascularization of the central nervous system coincides with formation of neuronal compartments during development (Paredes et al., 2018). Notably, blood vessels and their constituent endothelial cells support neuronal migration in the following ways: (1) supplying oxygen and nutrients; and (2) providing physical scaffolds that secrete chemoattractive/trophic factors providing a microenvironment that fosters neuroblast migration (Fujioka et al., 2019; Karakatsani et al., 2019; Tata and Ruhrberg, 2018). Recent analyses of human postmortem tissue revealed unique migratory streams in neonates persisting through infancy: (1) medial migratory stream; and (2) a collection of streams termed "Arc" supplying late-arriving interneurons to the frontal lobe, including the vPFC and cingulate cortices, respectively (Paredes et al., 2016a; Sanai et al., 2011). Yet the cellular processes enabling these unique migratory routes over vast distances remain elusive largely because of difficulties in acquiring scarce neurotypical human postmortem tissue during these early epochs of life; therefore, it is necessary to identify suitable animal model organisms as an alternative to address these questions.

Neonatal piglets are a close bioequivalent to humans, as they share similarities in gyrification, physiology, immunology, and anatomy. It was recently demonstrated that newborn piglet brains possess comparable migratory

streams, which provide the frontal lobe with newborn interneurons (Morton et al., 2017). As these cells are challenged with long migratory routes through a cytoarchitectural landscape similar to that of humans, in this work we evaluated their potential embryonic and postnatal origins, cortical destinations, and preferred cellular substrates from birth through toddlerhood. We found that neuroblasts are closely associated with blood vessels and astrocytes during migration, as opposed to isolated chain migration. Molecular profiling revealed that these migratory streams are largely composed of immature neocortical interneurons derived from the medial ganglionic eminence and caudal ganglionic eminence (CGE). Lastly, we determined that many of these neuroblasts were born postnatally.

RESULTS

Developmental timeline and study design

Larger mammalian species have emerged as ideal translational animal models for cell-dynamic studies of human brain development (Fernandez-Flores et al., 2018; La Rosa et al., 2018; Low et al., 2013; Parolisi et al., 2017). Key neuronal niches lining the SVZ of the postnatal porcine brain resemble those reported in humans, including cytoarchitectural lamination and robust migration of neuroblasts following birth (Morton et al., 2017; Paredes et al., 2016a). In addition, numerous streams—seen as round clusters in orthogonal planes—of migrating neuroblasts were identified within the piglet SVZ oriented toward the cortex (Morton et al., 2017). Piglets possess a highly evolved gyrencephalic neocortex, similar distribution of white matter (WM), and share key developmental trajectories similar to those in humans (Conrad et al., 2012; Costine et al., 2015). In contrast to the typical 40 weeks gestational period of humans, pig gestation requires ~114 days. In terms of brain development, longitudinal MRI studies have concluded that each week of pig brain development is the human equivalent of 1 month (Conrad et al., 2012, Conrad and Johnson, 2015; Jelsing et al., 2006). Thus, we evaluated multiple developmental stages including birth (postnatal day 0 [P0]), infancy (P16), toddlerhood (P42), and childhood (6 months) beginning with assessments in four subregions of the SVZ: anterior-end (AE)-, anterior (A)-, middle (M)-, and posterior (P)-SVZ (Figures 1A–1D).

Spatiotemporal distribution and numbers of DCX$^+$ neuroblast clusters in the postnatal porcine SVZ

The boundary of the SVZ was easily recognizable with distinct anatomical features: (1) opening of the lateral ventricle; (2) lining of the corpus callosum dorsally; and (3) head of the caudate nucleus inferiorly (Figures 1G–1R). No significant differences were found in the total number of doublecortin-positive (DCX$^+$) neuroblast clusters between age groups throughout the entire SVZ (Figure 1E); notably, DCX$^+$ neuroblast clusters were in close proximity to IB4$^+$ blood vessels in all regions and ages assessed (Figures 1G–1R). DCX$^+$ neuroblast clusters were still detectable at lower levels at 6 months of age in the SVZ (Figures S1A–S1D); however, they appeared less compact and organized. These data suggest that young piglets are endowed with an abundance of neuroblast clusters at birth, which may persist into adulthood as described in some larger mammalian species (Parolisi et al., 2017; Piumatti et al., 2018).

We next compared the frequency and distribution of neuroblast clusters throughout the SVZ. Compared with newborns (P0), the number of DCX$^+$ neuroblast clusters were significantly higher at P42 in the AE-SVZ, and at P16 And P42 in the A-SVZ (Figure 1G). A significant interaction between age and subregion was determined, indicating fewer DCX$^+$ neuroblast clusters at P16 compared with the P0 and P42 in the P-SVZ (Figure 1F). Collectively, these findings indicate that the piglet brain possesses a heterogeneous distribution of DCX$^+$ neuroblast clusters in the SVZ that are steadily maintained with age in a region-specific manner. Because a collective majority of neuroblasts clusters were found within the A- and M-SVZ (Figure 1F) and previous studies in piglets identified the A-SVZ as the most abundant source of neuroblasts capable of migrating to the frontal lobe at 2 weeks of age, we restricted our analyses to the A-SVZ at P16.

DCX$^+$ neuroblast clusters express markers of migration in the porcine SVZ during postnatal development

DCX$^+$ neuroblast clusters co-expressed polysialylated neuronal cell adhesion molecule (PSA-NCAM) within the SVZ, indicative of migratory neuroblasts (Figures 2A–2E; Wang et al., 2011); however, few DCX$^+$PSA-NCAM$^-$ cells within the neuroblast clusters were also seen. DCX$^+$PSA-NCAM$^+$ cells were also detectable in the corpus callosum, caudate nucleus, dorsal-lateral PFC, and anterior PFC. DCX$^+$ cells with an elongated cell body displaying bipolar morphology as well as a forked leading process in the caudate and WM tracts were frequent (Figures S2A and S2B). DCX$^+$ cells displayed varying morphology depending on spatial organization, including elongated cell bodies with long bipolar processes (in WM and putamen), larger cells with oval-shaped cell bodies with occasionally ramified apical dendrite arborizations (layer II of cortex), and tightly compact as well as small dispersed clusters (SVZ, WM). Multiple tightly associated-DCX$^+$ neuroblast clusters at P16 were observed extending out of the Arc-like AE-SVZ. DCX$^+$ neuroblast clusters protruding from the AE-SVZ were in streams spanning the striatum and oriented toward the insular

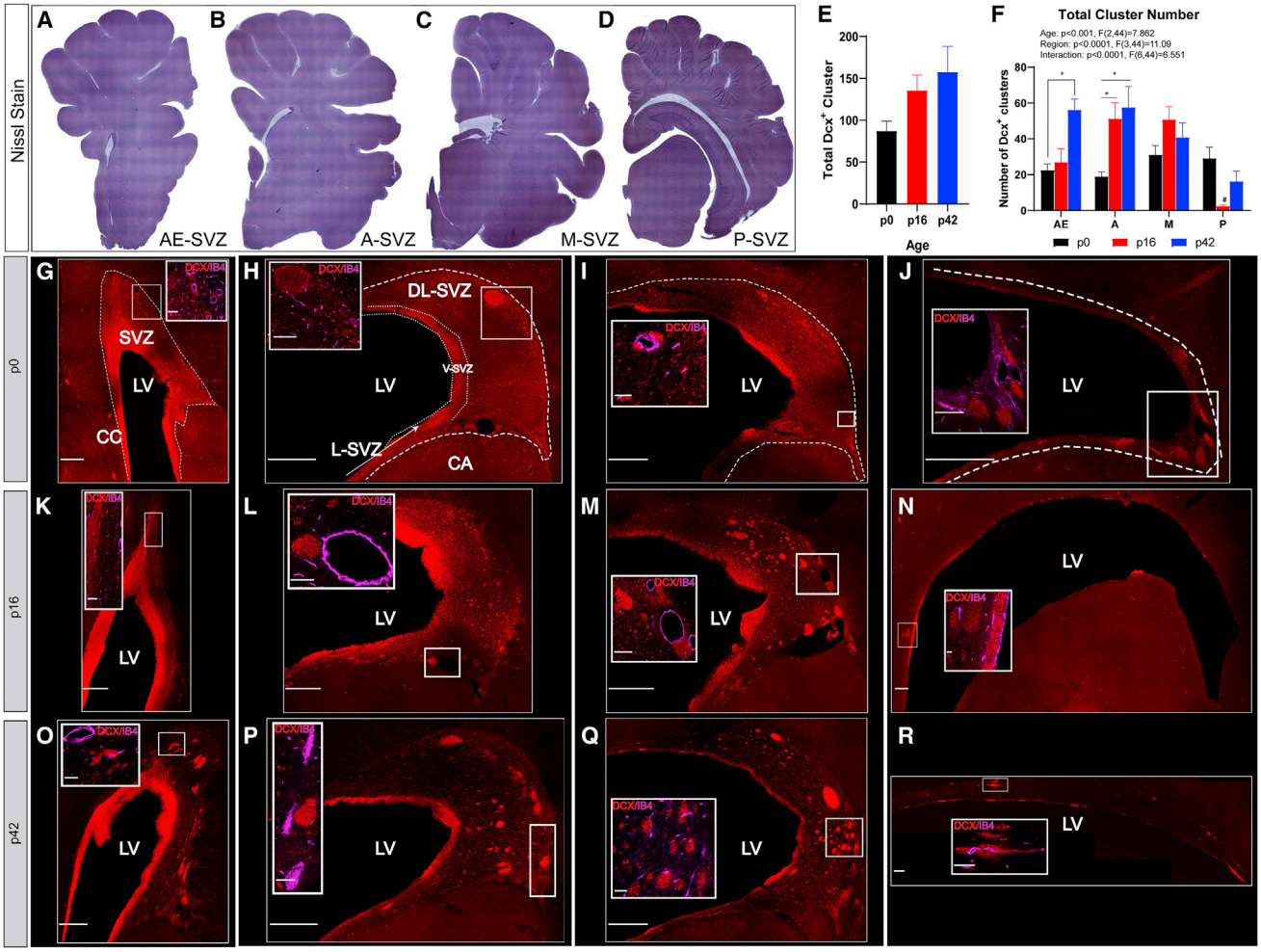

Figure 1. Development-related changes in the occurrence and regional distribution of neuroblast clusters throughout the piglet SVZ

(A–D) Cresyl violet staining on coronal sections of the SVZ at four anterior-posterior brain levels at 2 weeks of age.

(E) Quantification of the number of DCX$^+$ neuroblasts present in the SVZ (n = 6 animals, P0; n = 4 animals, P16; n = 4 animals, P42).

(F) Quantification of the number of DCX$^+$ neuroblasts in the four SVZ subregions at P0, P16, And P42.

(G–R) Spatiotemporal distribution of DCX$^+$ neuroblasts in coronal sections; between birth and 42 days, DCX$^+$ neuroblasts appear to have migrated from the posterior SVZ toward the rostral regions (A-SVZ) and in number with age. Higher-magnification images of boxed areas show DCX$^+$ neuroblasts close to IB4$^+$ blood vessels in four SVZ rostrocaudal regions at P0, P16, and P42. CC, corpus callosum; LV, lateral ventricle; V-SVZ, ventricular-subventricular zone; SVZ, subventricular zone; DL-, dorsal-lateral; L-, lateral.

Data are expressed as mean ± SEM. *p < 0.05, $^{\#}$p < 0.0001, one-way ANOVA with Bonferroni post hoc comparisons (E), ANOVA with Bonferroni post hoc test (F). Scale bars, 500 μm (insets, 100 μm).

cortex (Figure S3). DCX$^+$ neuroblast clusters rarely expressed the proliferative marker, Ki67 (Figures 2F and 2G), or the mature neuronal marker, NeuN (Figure 2H). Altogether, these data demonstrate that DCX$^+$ neuroblast clusters in the postnatal SVZ are likely migrating neuroblasts.

Mixed presence of postnatally derived neuroblasts within the SVZ and PFC

To determine whether neuroblasts were generated postnatally, we employed a bromodeoxyuridine (BrdU) pulse-chase experiment starting at P2 (Figures 3, S4, and S5). We labeled cells proliferating (Ki67$^+$) at the time of sacrifice in key regions (Figure 3B): (1) PFC, insular cortex, and respective subcortical WM; (2) AE-SVZ and genu corpus callosum (gCC); and (3) A-SVZ and the body of the corpus callosum (bCC). BrdU$^+$DCX$^+$ and BrdU$^+$Ki67$^+$cell density was quantified at 2 h post injection, 5 days post injection (dpi), and 14 dpi (Figures 3C–3H and S4C). BrdU$^+$DCX$^+$ neuroblasts were easily identifiable within the corpus callosum (CC) (Figures S4A and S4B) and the WM underlying

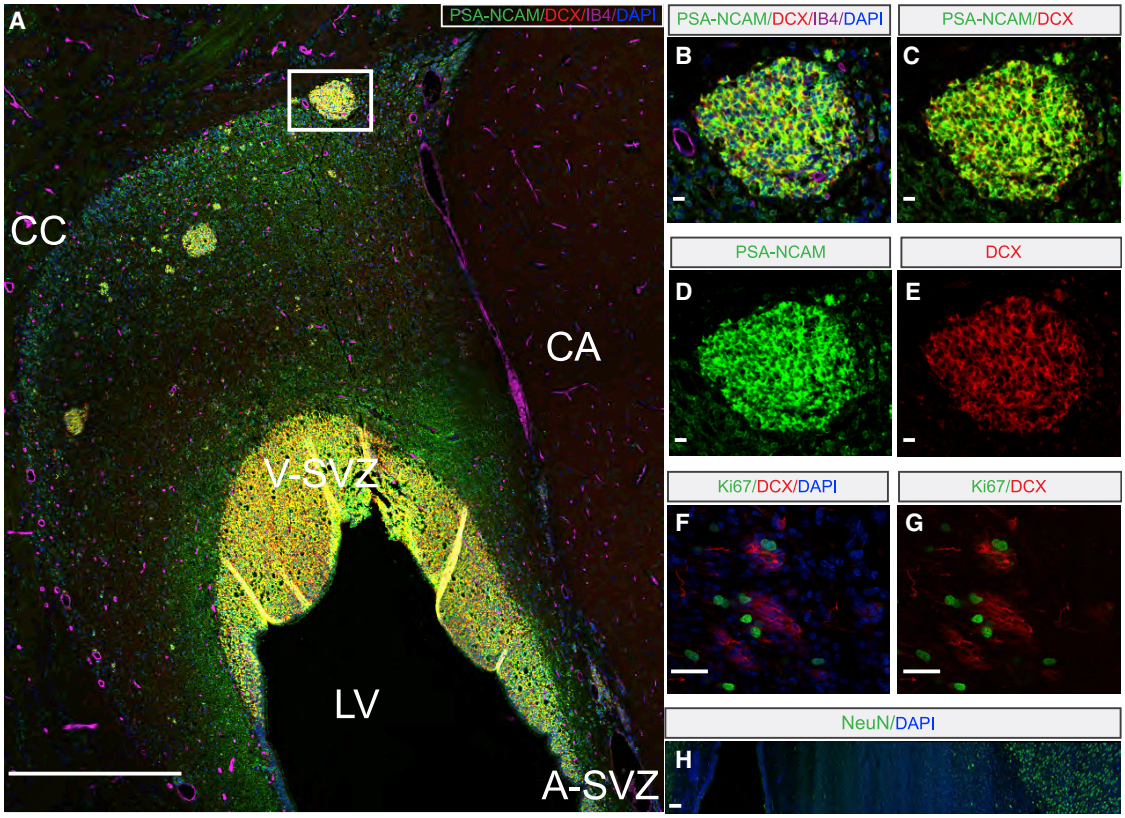

Figure 2. Postnatal neuroblast clusters express markers indicative of migration

(A) Low-magnification image of a coronal section illustrating subpopulations of DCX$^+$ neuroblasts in the A-SVZ, showing co-expression with PSA-NCAM at 2 weeks of age. CC, corpus callosum; CA, caudate nucleus; LV, lateral ventricle; V-SVZ, ventricular-subventricular zone. Scale bars, 500 μm.

(B–E) Higher-magnification images of DCX$^+$ PSA-NCAM$^+$ neuroblasts, annotated by white box. DAPI and IB4 immunostains. Scale bars, 10 μm.

(F and G) Piglet A-SVZ immunostained for cell proliferation marker, Ki67. Cell nuclei were stained with DAPI. Scale bars, 100 μm.

(H) Immunostain of DCX$^+$ neuroblasts and the postmitotic neuronal marker NeuN. Scale bar, 100 μm.

the insular cortex (Figure S5) often displaying a leading process from an elongated cell body. BrdU$^+$DCX$^+$ cells were within the PFC and insular cortex at all ages assessed (Figure 3C). Within the AE- and A-SVZ there were few BrdU$^+$DCX$^+$ cells relative to the total population of BrdU$^+$ cells 2 h following administration; by 5 and 14 dpi, an abundance of BrdU$^+$DCX$^+$ neuroblasts including a presence within neuroblast migratory clusters was evident (Figures 3E and 3F). We found limited cell proliferation spanning layer II/III of the PFC and insular cortex at birth (Figure S6) and 2 h post BrdU administration (Figure 3C).

Quantification revealed significant differences in the number of BrdU$^+$DCX$^+$ and BrdU$^+$Ki67$^+$cells relative to region and a significant difference in BrdU$^+$Ki67$^+$cells relative to age across the cortex and SVZ (Figures 3G and 3H). In addition, a significant difference was seen relative to age in BrdU$^+$DCX$^+$ cell density in the WM regions assessed (Figure S4). An increase in BrdU$^+$DCX$^+$ cells and BrdU$^+$Ki67$^+$ cells was visibly notable in the insular compared with the PFC at 5 dpi (Figures 3C, 3D, 3G, and 3H). Unlike the AE-SVZ, a significant peak in the number of BrdU$^+$DCX$^+$ cells was seen in the A-SVZ at 5 dpi compared with the 2 h and 14 dpi time points (Figure 3G). In addition, a significant decline in BrdU$^+$Ki67$^+$ cell numbers was seen over time following the first injection (P2, 2 h post injection) in both the AE- and A-SVZ (Figure 3H). Within the WM, there was a significant increase in the number BrdU$^+$DCX$^+$ cells at 5 dpi compared with the 2 h time point (Figure S4C). Lastly, a significant increase in the number of BrdU$^+$DCX$^+$ cells was seen in the bCC at 5 and 14 dpi compared with 2 h post injection. A decline in BrdU$^+$Ki67$^+$ cells in the SVZ concurrent with an increase in BrdU$^+$DCX$^+$ cells in WM tracts over time may suggest a postnatal emigration of newborn neuroblasts labeled as early as 2 days of age. In addition, the more mature

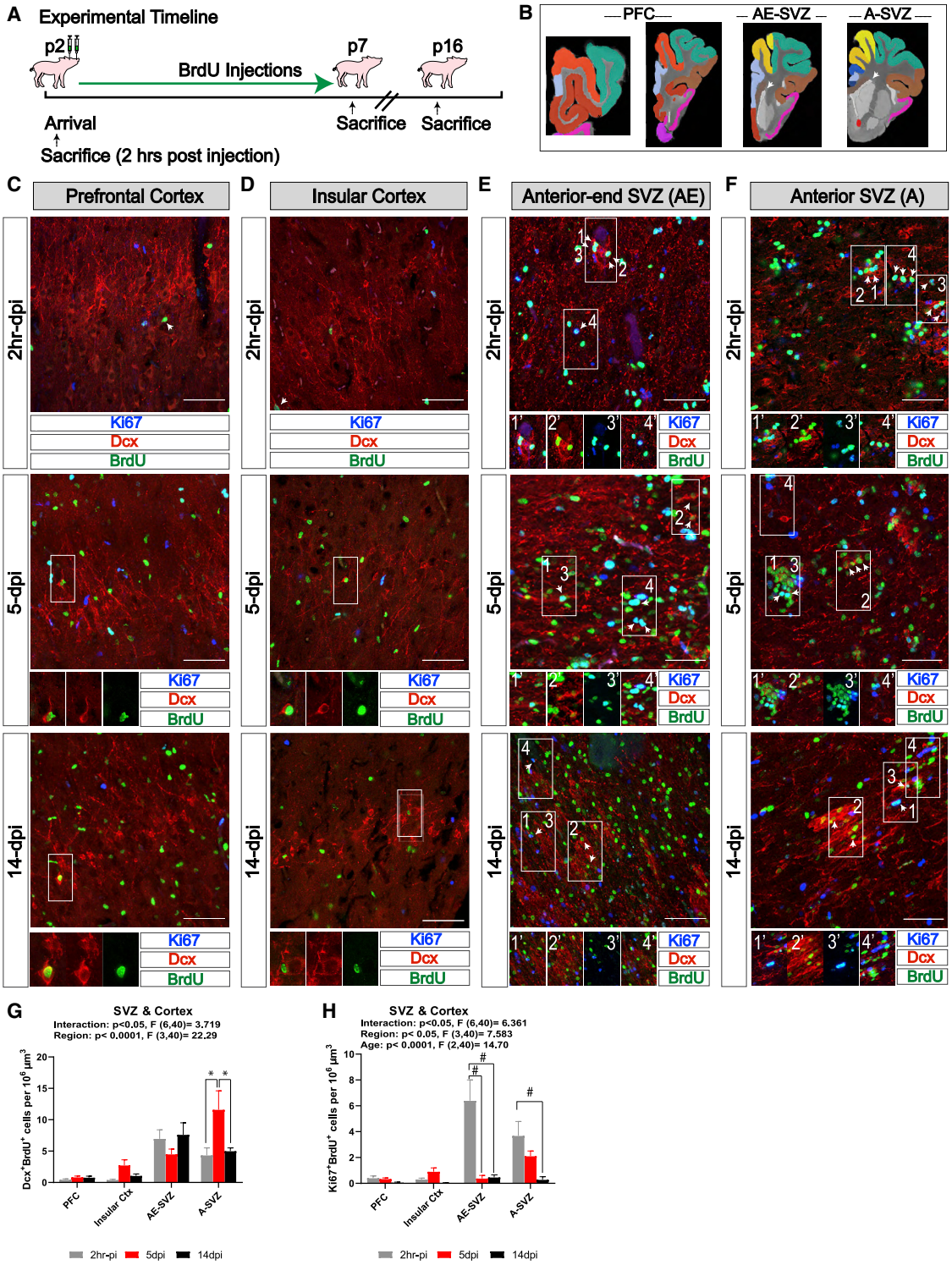

Figure 3. Mixed presence of postnatally derived neuroblasts within the SVZ and cortex

(A) BrdU was injected intraperitoneally into piglets once or twice daily for 5 days; animals were sacrificed 2 h post injection and at 5 and 14 days post injection.

(B) Axial scans of pig brain from a color-coded swine brain atlas, mapping regions of interest; white arrows mark the SVZ. Maroon, anterior prefrontal cortex; light blue, dorsal anterior cingulate cortex; red, dorsolateral prefrontal cortex; light brown, insular cortex; dark brown, corpus callosum.

(legend continued on next page)

morphology of BrdU$^+$DCX$^+$ cells in the cortex (Figures 3C and 3D) at 5 and 14 dpi is in line with our previous findings that focally labeled neuroblasts within the postnatal SVZ do provide the PFC and insular cortex with newborn neurons (Morton et al., 2017). Altogether, these findings suggest that a subset of the BrdU$^+$DCX$^+$ neurons observed outside of the SVZ at P7 (5 dpi) and P16 (14 dpi) are not generated locally.

SVZ-derived migrating neuroblast clusters are largely composed of young GABAergic interneurons in the postnatal piglet brain

Neurogenic niches established during embryogenesis within the ventral subpallidum (ganglionic eminences [GE]) appear to be preserved until adulthood in the SVZ (Paredes et al., 2016a; Parnavelas et al., 2002; Rakic, 1988). Spatial organization of progenitor cells within the GE selectively express transcription factors that correspond to distant neuronal subtypes. DCX$^+$ neuroblast clusters at P16 expressed the main inhibitory neurotransmitter γ-aminobutyric acid (GABA) (Figures 4A–4C). Within the A-SVZ at P16, neuroblast clusters expressed the calcium binding protein, secretagogin (SCGN)$^+$ associated with the caudal GE, which are selectively present in human cortical interneurons but not rodents (Raju et al., 2018). Individual cells within the clusters expressed markers of interneuron subclasses including parvalbumin and calretinin (Figures 4D and 4E). We identified a neuropeptide Y (NPY)-positive interneuron (Figure 4F). We observed a small population of parvalbumin (PV)$^+$calretinin (CalR)$^+$ cells within the clusters (Figure 4G), an observation previously reported from large-brained gyrencephalic species, including humans (Hashemi et al., 2017; Leuba and Saini, 1997; Yan et al., 1995). All subtypes of interneurons assessed were clearly visible within the upper layers of the prefrontal cortex during an epoch of circuitry refinement (Figures 4H and 4I). Reports have shown co-expression of SCGN$^+$ interneurons with Sp8, a marker associated with CGE/LGE origins (Ellis et al., 2019; Raju et al., 2018). Within the A-SVZ of P16 piglets there was robust co-expression of DCX$^+$ neuroblast clusters with SCGN and Sp8 (Figures 4J–4M). DCX$^+$Sp8$^+$SCGN$^+$ cells were also observed in the upper layers of the PFC (Figure 4N). Taken together, our results indicate that neuroblast clusters in the SVZ are young migrating GABAergic interneurons, partly derived from specific subregions of the GE that are destined to populate the postnatal neocortex.

Migrating neuroblasts are closely associated with cellular substrates

In human infants, large numbers of neuroblasts have been documented in close association with astrocytes and blood vessels potentially serving as scaffolds to facilitate migration (Paredes et al., 2016a). To visualize the association of cellular substrates near the surface of migrating neuroblast clusters, we generated a three-dimensional (3D) segmentation and rendering of immunolabeled clusters (Figures 5A and 5B); an axial image generated from the 3D porcine atlas (Saikali et al., 2010). Within the dorsal-lateral SVZ, DCX$^+$ neuroblast clusters were encased in GFAP$^+$ astrocytic processes that appeared to be mostly aligned in the directionality (tangentially) of migration (Figure 5C). Neuroblast clusters were observed directly contacting blood vessels in the A-SVZ, presumably utilizing them as a migratory substrate (Figure 5D). Analysis of the average distance between clusters and vessels displayed a significant increase with age (Figure 5E). However, with age DCX$^+$ clusters are less compact (see Figure S1) as well as undergoing vasculature structure changes (i.e., diameter, density, and tortuosity) (Zhao et al., 2021), suggesting that the change in distance of clusters and blood vessels is in part due to fewer existing clusters near vessels to facilitate vasophilic migration. We found that a majority of the DCX$^+$ neuroblast clusters are within 0–20 μm distance of a blood vessel (Figure 5F). This suggests that as the brain develops, there is less association between streams of migratory neuroblasts and vascular substrates within the SVZ.

Quantification of the number of neuroblast clusters associated with astrocytes and blood vessels revealed that their number and association with astrocytes was significantly higher at birth compared with blood vessels at all ages from P0 to P42 (Figure 5G). There were no significant differences in their association with blood vessels across ages. We found a significant increase in the number of neuroblasts associated with astrocytes across development in the AE-SVZ. The same was seen in the A-SVZ at P0 compared with P42 (Figure 5H), suggesting that these chains of neuroblast clusters are directed toward the OB through glial tubes as this sensory modality develops. We found a significant increase in the association between DCX$^+$ neuroblast clusters and blood vessels within the A-SVZ from P0 to P42. In the P-SVZ, at P0 there was a significant reduction in the amount of DCX$^+$ neuroblast clusters associated with blood vessels compared with P16 (Figure 5I). DCX$^+$ neuroblast clusters appeared heterogeneous in size (Figure 5J), and

(C–F) Immunostains of BrdU, DCX, and Ki67 within the prefrontal cortex (PFC), insular cortex (ctx), anterior-end SVZ (AE-SVZ), and anterior SVZ (A-SVZ) at three time points/ages. Scale bars, 100 μm. Insets mark high magnification of numbered panels beneath respective images.

(G and H) Quantification of BrdU$^+$/DCX$^+$ (G) and BrdU$^+$/Ki67$^+$ (H) cells within the different brain regions assessed. Data are expressed as mean ± SEM, n = 4–5 animals/group. *$p < 0.05$, $^{\#}p < 0.0001$, two-way ANOVA with Bonferroni post hoc comparison.

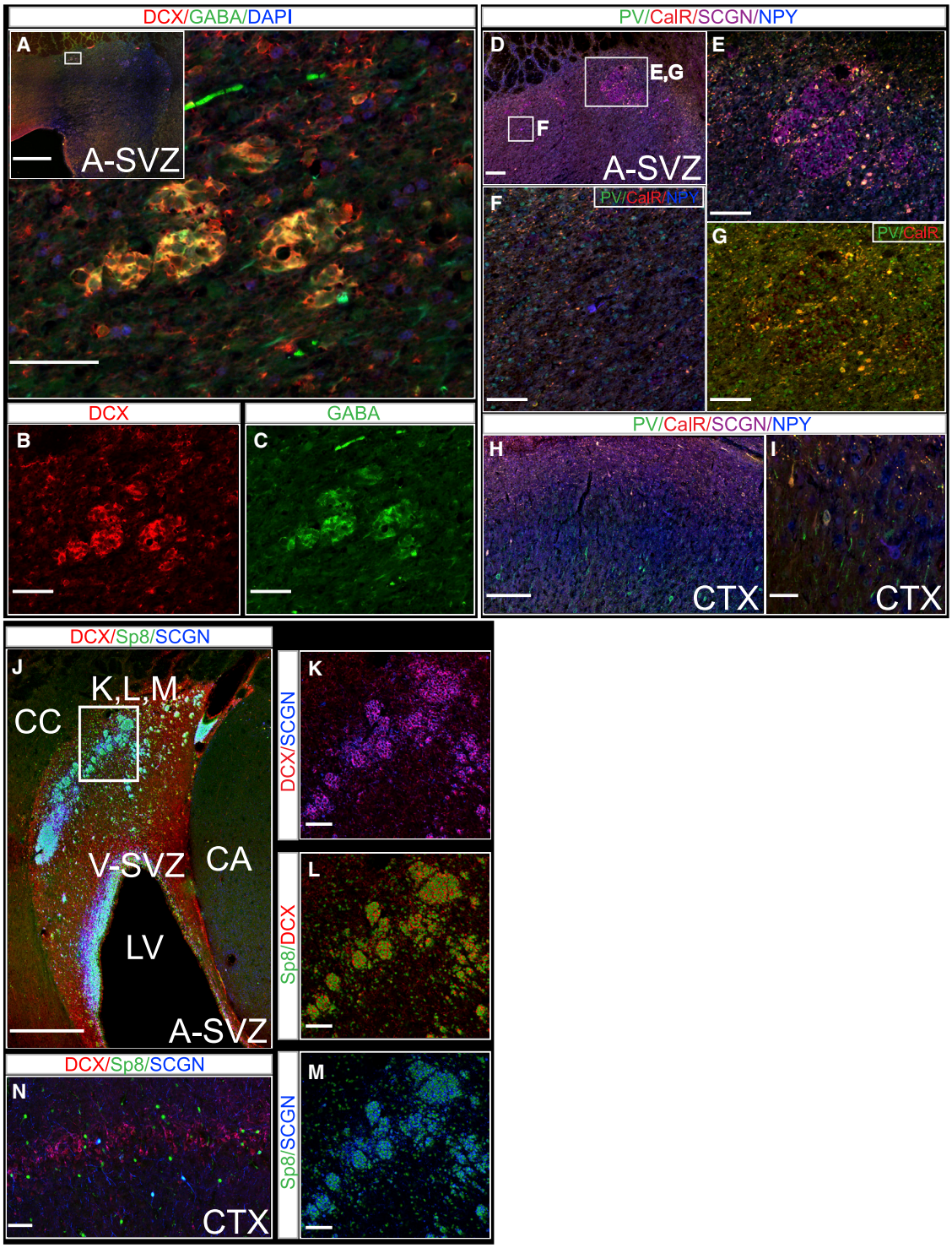

Figure 4. Detection of interneuron and subpallial marker expression in migrating neuroblasts within the SVZ of postnatal piglets

(A–C) At 2 weeks of age, many of the migrating DCX$^+$ neuroblasts in the A-SVZ express the inhibitory neurotransmitter GABA. Scale bars, 100 μm (inset, 500 μm).

(D–G) (D) Subpopulations of DCX$^+$ neuroblasts/cells in the A-SVZ (regions noted in E, F, G) co-express interneuron subtype markers parvalbumin (PV), calretinin (CalR), or neuropeptide Y (NPY). Scale bars, 100 μm (D) and 50 μm (E–G).

(H and I) PV$^+$, CalR$^+$, NPY$^+$, and SCGN$^+$ interneurons in the upper cortical layers I and II/III. Scale bars, 100 μm.

(legend continued on next page)

the majority of the clusters in the A- and M-SVZ across ages appeared to be smaller than their partner vessels (Figure 5K). From these data, we concluded that the extent of neuroblast association with glial and blood vessel substrates corresponded to the postnatal changes in distribution of neuroblast clusters across SVZ subregions.

Postnatal expression of SCGN$^+$Sp8$^+$DCX$^+$ neuroblast clusters associated with blood vessels in the porcine SVZ

In the A-SVZ of P0 and P16 piglets, each DCX$^+$ cluster co-expressed SCGN and Sp8 (Figures 6A–6E). At birth, the percentage of co-localization between DCX and SCGN varied from that seen in DCX$^+$Sp8$^+$ clusters. The association of DCX$^+$SCGN$^+$ clusters with blood vessels appeared to be similar throughout development, compared with DCX$^+$Sp8$^+$ clusters. The percentage of co-localized clusters increased with age in both groups, and the percentage of migrating DCX$^+$SCGN$^+$ clusters that were not in contact with blood vessels was almost identical to that of DCX$^+$Sp8$^+$ clusters during the early postnatal period (Figures 6F and 6G). These findings suggest that during critical periods of postnatal development, migrating neuroblasts destined to become cortical GABAergic interneurons preferably associate with blood vessels.

DISCUSSION

In recent years, investigation into postnatal neurogenesis has revealed detailed characterization of late-arriving streams of newborn neurons populating multiple cortical regions in large species. However, there are cross-species variations in neurogenesis yielding an incomplete picture. A handful of reports have suggested a persistence in postnatal neurogenesis providing interneurons to the cortex throughout life (mice: Inta et al., 2008 and Le Magueresse et al., 2012; rabbit: Luzzati et al., 2003 and Ponti et al., 2006; ferret: Ellis et al., 2019; human tissue: Sanai et al., 2011 and Paredes et al., 2016a). Yet emerging data also suggest the potential for co-existence between newborn neurons and non-newly generated neurons (prior to birth) within non-neurogenic brain regions (Sorrells et al., 2019). Owing to closely shared features of postnatal neurogenesis among large-brained, gyrencephalic mammalian species, the question arises as to whether the piglet possesses the postnatal characteristics of neurogenesis and neuroblast migration seen in humans.

The neurogenic niche within the SVZ has been previously shown to generate a small number of NSPCs endogenously after birth that continue to proliferate and maintain neurogenic potential into adulthood, enabling neural circuit plasticity (Sanai et al., 2011; Bond et al., 2015). In parallel, evidence from human infant brains has shown that neuroblasts migrate to reach the frontal lobe, suggesting a further postnatal contribution to corticogenesis (Paredes et al., 2016a). In addition, previous findings from focally labeled cells within the porcine SVZ demonstrated neuroblast migration to the frontal lobe followed by maturation into interneuron subtypes (Morton et al., 2017). In agreement with the previous findings of developmental markers for structural plasticity and neuronal migration that transcend typical age-related expression patterns, our current immunohistochemical analysis revealed that the vast majority of DCX$^+$ cells in the neuroblast clusters of the postnatal porcine SVZ expressed the migratory marker PSA-NCAM (Figures 2A–2E) but did not express Ki67 (Figures 2F and 2G) or NeuN (Figure 2H). Moreover, we observed populations of DCX$^+$/NeuN$^-$ neuroblast clusters in the WM tracts of the striatum of the P16 piglet oriented toward the insular cortex. Considering that Ki67 and NeuN are necessary for cell proliferation and neuronal maturation, respectively, it appears that porcine SVZ-derived neuroblasts are young migratory neurons. Our observations in conjunction with evidence from preserved subpopulations of immature neurons throughout various cortical regions, WM, and SVZ-like region of cetaceans and mammals, implies that in the porcine SVZ, late waves of young migratory neuroblasts may be a source for new neurons that integrate into the existing cortical circuitry during postnatal life (La Rosa et al., 2018; Parolisi et al., 2017; Piumatti et al., 2018).

Current literature suggests that within gyrencephalic large-brained mammalian species, structural brain plasticity seems to be refined and maintained during postnatal development through a source of non-newly generated "immature" neurons that remain following birth (generated embryonically) (extensively reviewed in Palazzo et al., 2018; Bonfanti and Charvet, 2021; La Rosa and Bonfanti, 2021). It has been demonstrated across evolutionarily diverse large-brain mammalian species that these subpopulations of delayed immaturity neurons extensively populate layer II of the neocortex (Piumatti et al., 2018 [sheep]; La Rosa et al., 2020 [cats and chimpanzees]), but are limited to the paleocortex in rodents (Gómez-Climent et al., 2008). One notable consideration in cross-species comparisons is the timing of key milestones during brain

(J) Individual DCX$^+$ clusters express the regional transcription factor Sp8 specifying ventral telencephalic origin. Scale bars, 500 μm.
(K–M) DCX$^+$ neuroblasts co-express SCGN and Sp8 in the A-SVZ. Scale bars, 100 μm. Magnified images from the location marked by inset in (J).
(N) Individual cells express DCX$^+$ SCGN$^+$, and Sp8$^+$ in the upper layers of the prefrontal cortex.
CC, corpus callosum; CA, caudate nucleus; LV, lateral ventricle; V-SVZ, ventricular-subventricular zone.

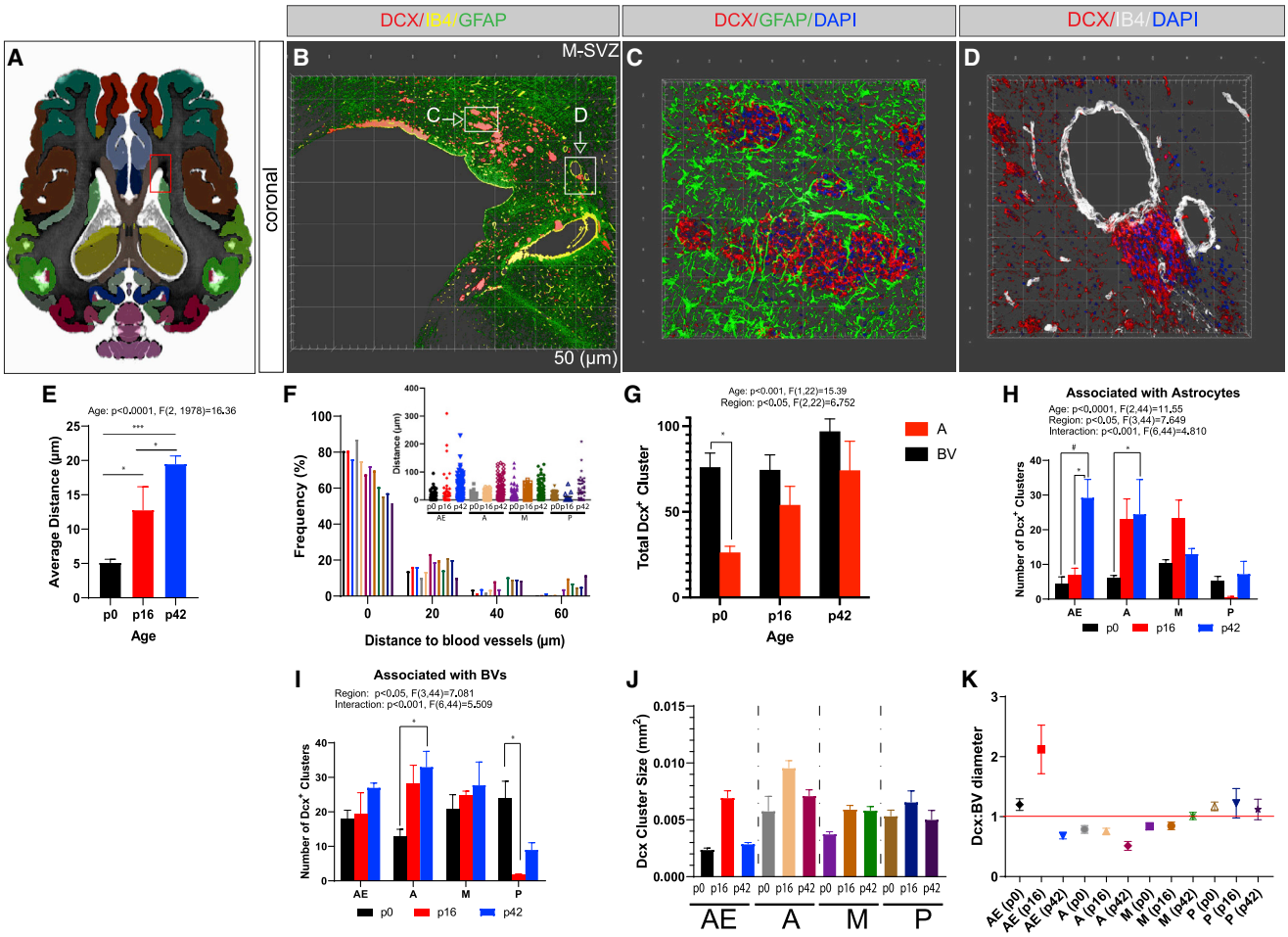

Figure 5. Migrating neuroblasts are commonly associated with cellular substrates in the SVZ of neonates

(A) Axial scan of pig brain from swine brain atlas; red box, location of A-SVZ. Cortices are color coded: red, dorsal prefrontal; dark green, primary somatosensory; brown, insular; light green, auditory; gray, middle temporal gyrus; burgundy, associative visual; forest green, parahippocampal; purple, cerebellum.

(B) 3D-reconstructed image of the M-SVZ immunolabeled with DCX, IB4, and GFAP on the coronal plane.

(C and D) 3D segmentation of DCX^+ neuroblasts within the SVZ marked by insets in (B), illustrating DCX^+ neuroblasts encased in $GFAP^+$ astrocytic processes (C), and intimately associated with $IB4^+$ blood vessels (D).

(E) Quantification of the average distance of between DCX^+ clusters and blood vessels.

(F) Frequency distribution of DCX^+ neuroblast cluster-to-vessel distance measured from the edge of each cluster to its nearest neighboring the entire SVZ. Inset shows the quantitated average of cluster-to-vessel distance within SVZ subregions.

(G) Quantification of the number of DCX^+ clusters in association with $GFAP^+$ astrocytic processes or $IB4^+$ blood vessels between birth and 42 days of age.

(H and I) Quantification of the number of clusters associated with astrocytes (H) or blood vessels (I).

(J) Size of DCX^+ neuroblasts measured throughout the entire SVZ at different ages.

(K) Size correlation between blood vessel and DCX^+ neuroblast cluster diameter.

Data are expressed as mean ± SEM, n = 4–6 animals/group. $^*p < 0.05$, $^{\#}p < 0.001$, $^{***}p < 0.0001$, one-way ANOVA with Bonferroni post hoc comparisons (E), two-way ANOVA with Bonferroni post hoc comparisons (G–J).

development versus the timing of other biological processes such at the onset of puberty. Our study focused on ages equivalent to key periods during postnatal development up to a 6-month-old human equivalence in brain development; however, it should be noted that pigs reach sexual maturity at 6 months of age whereas humans reach puberty during adolescence. Although our analyses at this 6-month time point were limited and qualitative, future studies probing sexual dimorphisms will be of great insight.

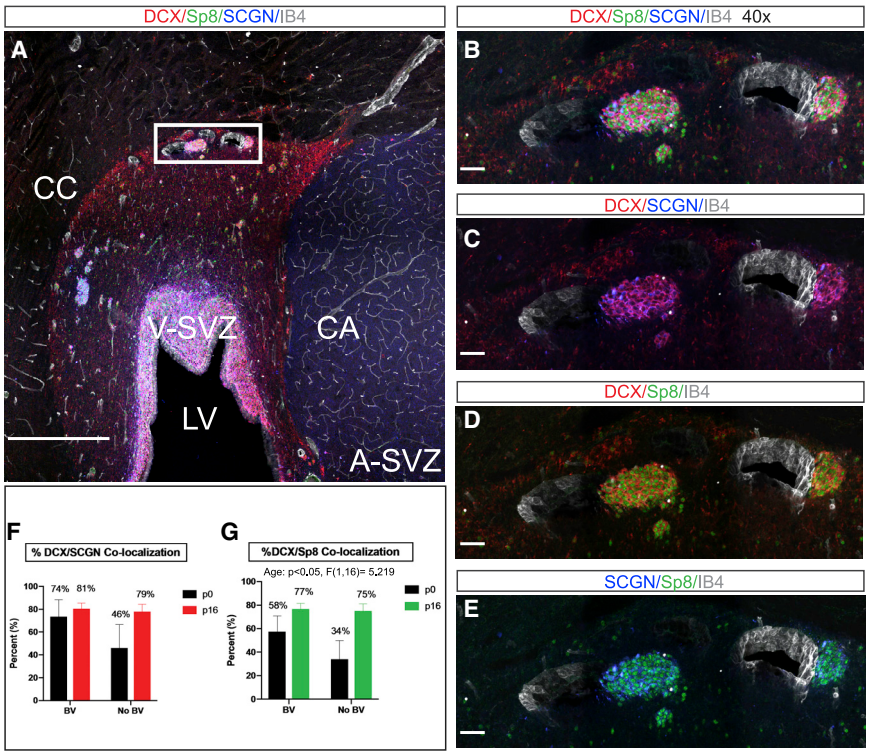

Figure 6. A majority of DCX$^+$ neuroblast clusters co-localize with SCGN and Sp8 in the piglet SVZ

(A) DCX, Sp8, SCGN, IB4 immunolabeled coronal section at 2 weeks of age, illustrating the contact between neuroblast clusters and blood vessels in the A-SVZ. Scale bar, 500 μm.

(B–E) Higher-magnification images of DCX$^+$Sp8$^+$SCGN$^+$ clusters. Scale bars, 100 μm.

(F and G) Quantification of co-localization with SCGN (F) or Sp8 (G) in the presence and absence of vessel association. Data are expressed as mean ± SEM, n = 4–6 animals/group, two-way ANOVA with Bonferroni post hoc test.

CC, corpus callosum; CA, caudate nucleus; LV, lateral ventricle; V-SVZ, ventricular-subventricular zone.

By utilizing the gyrencephalic cortex of the porcine brain as a relatively high-order translational model organism, we accessed the postnatal genesis of DCX$^+$ cells within comparable brain regions of the cortex and subventricular zone (i.e., PFC, insular, AE-SVZ, and A-SVZ). In the present study, using pulse-chase labeling of BrdU and a pan-cell proliferation marker (Ki67), we revealed the occurrence of doubled stained BrdU$^+$/DCX$^+$ cells born postnatally in several regions of the brain (Figures 3, S4, and S5). While BrdU-labeled cells were abundantly visible within 2 h of administration, few examples of DCX$^+$ neuroblasts undergoing cell division were seen at this time in all regions assessed, including the SVZ. Quantification suggested that an abundance of newly generated neurons in the SVZ are en route, via underlying WM tracts, to populate the insular and frontal cortex. While the findings in the insular cortex and the respective WM tract were more striking, this is potentially due to the proximity to the SVZ compared with the relatively distant PFC; however, our quantitative results did not reach statistical significance in the cortex at the ages assessed. We acknowledge potential limitations encountered, including BrdU detection limitations following multiple rounds of cell division (Taupin, 2007) and a relatively short pulse chase. Therefore, future assessments at later ages would be informative. Previous work documenting the migration of interneurons in piglets was on a longer time scale (4 weeks) following focal injections into the SVZ (Morton et al., 2017); however, whether the interneurons were produced postnatally was not addressed. Paired with evidence of non-newly generated neuroblasts in other species, our findings are in support of a mixed population of immature neurons retained from embryonic periods and newly generated immature neurons during postnatal development that likely contribute to structural plasticity in a large mammalian species.

Here, we have shown that neuroblasts in the SVZ are encased by astrocytic processes and are preferentially associated with blood vessels (Figures 5A–5D). On the other hand, by P42, the number of neuroblasts encased by astrocytic processes was drastically increased in the rostral regions of the SVZ (Figures 5E–5I). The apparent increase in neuroblast-astrocyte interaction is similar to results from studies in postnatal mice and rats, in which the assembly of glial tubes and chain migration from the SVZ to the OB was detected by P21–P25 (Bozoyan et al., 2012; Peretto et al., 2005). Nevertheless, it has become more and more evident that SVZ-derived neuroblasts utilize vascular scaffolds not only for migration within the RMS-OB but also through the parenchyma as seen in postnatal rabbits, cerebral cortex as seen in mice, and the SVZ arc as seen in human infants (Bovetti et al., 2007; Inta et al., 2008; Le Magueresse et al., 2012; Paredes et al., 2016a; Ponti et al., 2006; Snapyan et al., 2009). Taking into account the close relationship between DCX$^+$ clusters and

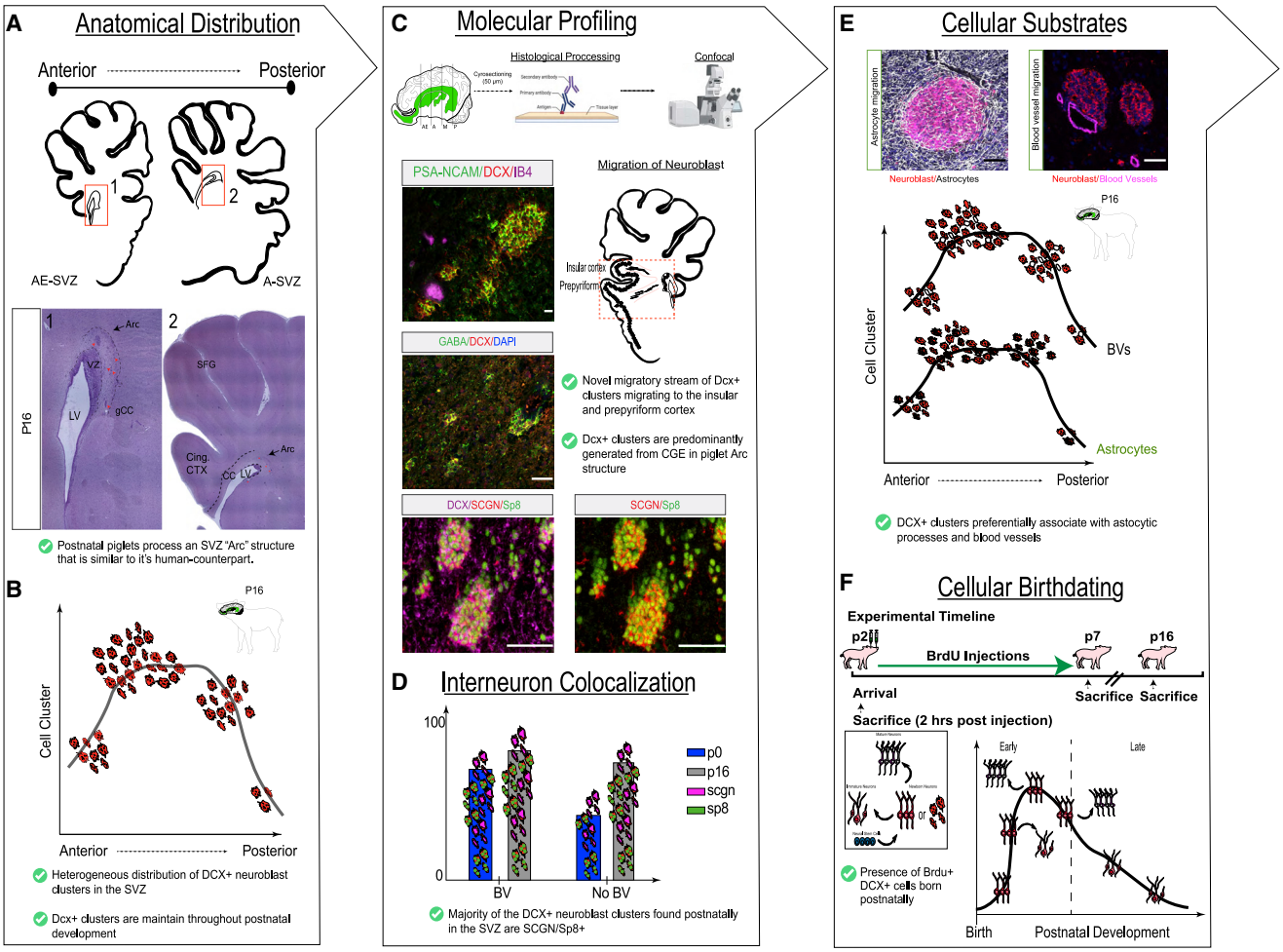

Figure 7. Schematic summary of the regional distribution and substrate characterization of neuroblasts in the postnatal piglet brain

The gyrencephalic piglet brain (A and B) possesses a robust Arc structure along the lateral ventricle at different SVZ locations as previously described in some large-brain mammalians including humans. Most of these neuroblasts (e.g., DCX^+ clusters) are maintained throughout postnatal development, and (C and D) co-express markers associated with migration (PSA-NCAM) that originated from the caudal ganglionic eminence (SCGN/Sp8). These neuroblasts clusters (E and F) were encased in astrocytic processes and preferentially associated with blood vessels in the SVZ. Additionally, newly generated neuroblasts ($BrdU^+DCX^+$) were detectable in brain regions of the cortex, white matter, and SVZ of the postnatal piglet brain. Current knowledge suggests that the postnatal piglet brain offers a suitable translational model system to study substrate-dependent neuroblast migration and the potential impact of pathological events on cortical development.

blood vessels in the developing human fetal brain, proximity to blood vessels may exacerbate vulnerability to pathological changes in blood flow, hypoxia, or hypoxia-ischemia, which would likely impact excitatory/inhibitory balance during the later stages of cortical growth.

The dynamic relationship between extended postnatal development and neocortical expansion remains to be understood (Stepien et al., 2021). Nevertheless, the overall distribution of postnatal DCX^+ neuroblasts might represent a large, heterogeneous population of undifferentiated neurons that serves as a parallel form of plasticity in large-brained mammals (Figure 7). This hypothesis is supported by the persistent occurrence of undifferentiated cells, postnatally, with morphology and cell marker expression patterns reminiscent of immaturity in larger expanded neocortices (Parolisi et al., 2017; Piumatti et al., 2018). Moreover, the migration modalities revealed here represent anatomical substrates which we infer SVZ-derived neuroblast clusters utilize for migration to the cortex in a substrate-dependent manner. Preferential association with the vascular system might also be important in terms of cortical maturation, as the vascular niche is a critical regulator of cellular function. Defects to neuron migration along blood vessels could result in immature cortical

development as implied in a swine model of congenital heart disease (Morton et al., 2017). Future studies focused on substrate migration from the postnatal SVZ in large animals may yield novel complex migratory streams that are yet to be discovered in the developing human brain.

EXPERIMENTAL PROCEDURES

Animals

Domestic, white (Yorkshire/Landrace) piglets were obtained from the Swine Agricultural Research and Extension Center at Virginia Tech. All experiments were conducted in accordance with the NIH Guide for the Care and Use of Laboratory Animals and performed under the approval of the Virginia Tech Institutional Animal Care and Use Committee.

Imaging

A Zeiss LSM 880 (Carl Zeiss Microscopy) or Nikon C2 confocal laser scanning microscopic system (Nikon Instruments, Melville, NY) was used in collecting tiled and high-resolution z-stacks for analyses following fluorescent immunohistochemical staining. Images were acquired with a 4×,10×, 20×, or 40× water objective. All images were acquired as 50-μm-thick sections. .nd2 and.czi files were covered to.sis files using Vision 4D software for further analyses. White light images were acquired at 4× on an Olympus BX51TRF microscope with MicroBrightField Stereoinvestigator software on 5-μm-thick sections.

Cell counting and quantification

Neuroblast cluster measurements

Exhaustive quantification of the number of DCX^+ clusters was analyzed on tiled z-stack projections spanning two levels of the SVZ (dorsolateral SVZ [DL-SVZ] and lateral SVZ [L-SVZ]) using Vision 4D software. The size of each cluster was determined by manually drawing polygonal contours and calculating the area (μm); approximations of cluster diameter were further calculated based on the area of a circle.

Neuroblast cluster analyses relative to the cellular substrate

Quantification of DCX^+ clusters near blood vessels and within astrocytic glial tubes was performed using Vision 4D software. In each SVZ area, the total number of DCX^+ clusters nearest to the blood vessels along with those surrounded by astrocytic processes were counted using Vision 4D software. The distance from each DCX^+ cluster to the nearest blood vessel was manually calculated by an experienced researcher using the ruler annotation function of Vision 4D software. Distances in micrometers were recorded, and data are presented as a histogram of the frequency of clusters relative to the distance to the substrate.

Neuroblast cluster co-localizations

Confocal images were taken from coronal slices (50 μm thickness) within the A-SVZ at 0, 16, and 42 days of age. Percent co-localizations were calculated by counting the number of co-localized cells and dividing by the total number of DCX^+ cell bodies per cluster using ImageJ software.

Statistical analyses

A two-tailed, unpaired Student's t test was performed for single comparisons; data were considered significantly different if $p < 0.05$. When two or more samples were being compared, statistical significance between groups was determined by two-way ANOVA with Bonferroni's post hoc multiple comparison test, whereby $p < 0.05$ determined significance. Data are expressed as mean ± SEM (SE of mean). GraphPad Prism software was used to run Student's t test and ANOVAs. Error bars in figures represent SEM, with $^{*}p \leq 0.05$, $^{***}p \leq 0.001$, and $^{\#}p \leq 0.0001$.

Data and code availability

All data are included in the manuscript and supplemental information.

SUPPLEMENTAL INFORMATION

Supplemental information can be found online at https://doi.org/10.1016/j.stemcr.2022.07.015.

AUTHOR CONTRIBUTIONS

P.D.M. designed the experiments. D.D.L.P. carried out experiments with assistance from S.N.H., S.A., A.L.R., C.G., and R.M. D.D.L.P. analyzed data. D.D.L.P. prepared the figures and wrote the report with P.D.M.

ACKNOWLEDGMENTS

We gratefully thank Drs. Sherrie Clark-Deener and Calvin Lau for their assistance with veterinary services. We are also thankful to Jessica Neary and Garrett Walker for assistance in animal husbandry. We also would like to thank Raymundo Hernandez, Beatriz Torres, Swagatika Paul, and Dr. Alicia Pickrell for technical advice. We would like to acknowledge Karen Hall and Rachel McNeil for animal care. This work was supported by the US National Institutes of Health (R15NS108183 to P.D.M.).

CONFLICTS OF INTEREST

The authors declare no competing interests.

Received: August 19, 2021
Revised: July 22, 2022
Accepted: July 23, 2022
Published: August 18, 2022

REFERENCES

Alvarez-Buylla, A., and Garcia-Verdugo, J.M. (2002). Neurogenesis in adult subventricular zone. J. Neurosci. *22*, 629–634.

Anton, E.S., Ghashghaei, H.T., Weber, J.L., McCann, C., Fischer, T.M., Cheung, I.D., Gassmann, M., Messing, A., Klein, R., Schwab, M.H., et al. (2004). Receptor tyrosine kinase ErbB4 modulates neuroblast migration and placement in the adult forebrain. Nat. Neurosci. *7*, 1319–1328.

Aoyagi, Y., Hibi, T., Kimori, Y., Sawada, M., Kawakami, R., Sawamoto, K., and Nemoto, T. (2018). Heterogeneous distribution of

doublecortin-expressing cells surrounding the rostral migratory stream in the juvenile mouse. J. Comp. Neurol. *526*, 2631–2646.

Azevedo, F.A.C., Carvalho, L.R.B., Grinberg, L.T., Farfel, J.M., Ferretti, R.E.L., Leite, R.E.P., Jacob Filho, W., Lent, R., and Herculano-Houzel, S. (2009). Equal numbers of neuronal and nonneuronal cells make the human brain an isometrically scaled-up primate brain. J. Comp. Neurol. *513*, 532–541.

Belvindrah, R., Hankel, S., Walker, J., Patton, B.L., and Müller, U. (2007). Beta1 integrins control the formation of cell chains in the adult rostral migratory stream. J. Neurosci. *27*, 2704–2717.

Bond, A.M., Ming, G.L., and Song, H. (2015). Adult mammalian neural stem cells and neurogenesis: five decades later. Cell Stem Cell *17*, 385–395.

Bonfanti, L., and Charvet, C.J. (2021). Brain plasticity in humans and model systems: advances, challenges, and future directions. Int. J. Mol. Sci. *22*, 9358.

Bovetti, S., Hsieh, Y.C., Bovolin, P., Perroteau, I., Kazunori, T., and Puche, A.C. (2007). Blood vessels form a scaffold for neuroblast migration in the adult olfactory bulb. J. Neurosci. *27*, 5976–5980.

Bozoyan, L., Khlghatyan, J., and Saghatelyan, A. (2012). Astrocytes control the development of the migration-promoting vasculature scaffold in the postnatal brain via VEGF signaling. J. Neurosci. *32*, 1687–1704.

Chazal, G., Durbec, P., Jankovski, A., Rougon, G., and Cremer, H. (2000). Consequences of neural cell adhesion molecule deficiency on cell migration in the rostral migratory stream of the mouse. J. Neurosci. *20*, 1446–1457.

Conrad, M.S., Dilger, R.N., and Johnson, R.W. (2012). Brain growth of the domestic pig (Sus scrofa) from 2 to 24 weeks of age: a longitudinal MRI study. Dev. Neurosci. *34*, 291–298.

Conrad, M.S., and Johnson, R.W. (2015). The domestic piglet: an important model for investigating the neurodevelopmental consequences of early life insults. Annu. Rev. Anim. Biosci. *3*, 245–264.

Costine, B.A., Missios, S., Taylor, S.R., McGuone, D., Smith, C.M., Dodge, C.P., Harris, B.T., and Duhaime, A.C. (2015). The subventricular zone in the immature piglet brain: anatomy and exodus of neuroblasts into white matter after traumatic brain injury. Dev. Neurosci. *37*, 115–130.

Ellis, J.K., Sorrells, S.F., Mikhailova, S., Chavali, M., Chang, S., Sabeur, K., McQuillen, P., and Rowitch, D.H. (2019). Ferret brain possesses young interneuron collections equivalent to human postnatal migratory streams. J. Comp. Neurol. *527*, 2843–2859.

Fernández-Flores, F., García-Verdugo, J.M., Martín-Ibáñez, R., Herranz, C., Fondevila, D., Canals, J.M., Arús, C., and Pumarola, M. (2018). Characterization of the canine rostral ventricular-subventricular zone: morphological, immunohistochemical, ultrastructural, and neurosphere assay studies. J. Comp. Neurol. *526*, 721–741.

Fujioka, T., Kaneko, N., and Sawamoto, K. (2019). Blood vessels as a scaffold for neuronal migration. Neurochem. Int. *126*, 69–73.

Gengatharan, A., Bammann, R.R., and Saghatelyan, A. (2016). The role of astrocytes in the generation, migration, and integration of new neurons in the adult olfactory bulb. Front. Neurosci. *10*, 149.

Gómez-Climent, M.A., Castillo-Gómez, E., Varea, E., Guirado, R., Blasco-Ibáñez, J.M., Crespo, C., Martínez-Guijarro, F.J., Nácher, J., and Nácher, J. (2008). A population of prenatally generated cells in the rat paleocortex maintains an immature neuronal phenotype into adulthood. Cereb. Cortex *18*, 2229–2240.

Hashemi, E., Ariza, J., Rogers, H., Noctor, S.C., and Martínez-Cerdeño, V. (2017). The number of parvalbumin-expressing interneurons is decreased in the prefrontal cortex in autism. Cereb. Cortex *27*, 1931–1943.

Inta, D., Alfonso, J., von Engelhardt, J., Kreuzberg, M.M., Meyer, A.H., van Hooft, J.A., and Monyer, H. (2008). Neurogenesis and widespread forebrain migration of distinct GABAergic neurons from the postnatal subventricular zone. Proc. Natl. Acad. Sci. USA *105*, 20994–20999.

Jelsing, J., Nielsen, R., Olsen, A.K., Grand, N., Hemmingsen, R., and Pakkenberg, B. (2006). The postnatal development of neocortical neurons and glial cells in the Gottingen minipig and the domestic pig brain. J. Exp. Biol. *209*, 1454–1462.

Kaneko, N., Marín, O., Koike, M., Hirota, Y., Uchiyama, Y., Wu, J.Y., Lu, Q., Tessier-Lavigne, M., Alvarez-Buylla, A., Okano, H., et al. (2010). New neurons clear the path of astrocytic processes for their rapid migration in the adult brain. Neuron *67*, 213–223.

Karakatsani, A., Shah, B., and Ruiz de Almodovar, C. (2019). Blood vessels as regulators of neural stem cell properties. Front. Mol. Neurosci. *12*, 85.

Kornack, D.R., and Rakic, P. (2001). The generation, migration, and differentiation of olfactory neurons in the adult primate brain. Proc. Natl. Acad. Sci. USA *98*, 4752–4757.

La Rosa, C., and Bonfanti, L. (2021). Searching for alternatives to brain regeneration. Neural Regen. Res. *16*, 2198–2200.

La Rosa, C., Cavallo, F., Pecora, A., Chincarini, M., Ala, U., Faulkes, C.G., Nacher, J., Cozzi, B., Sherwood, C.C., Amrein, I., and Bonfanti, L. (2020). Phylogenetic variation in cortical layer II immature neuron reservoir of mammals. Elife *9*, e55456.

La Rosa, C., Parolisi, R., Palazzo, O., Lévy, F., Meurisse, M., and Bonfanti, L. (2018). Clusters of DCX+ cells "trapped" in the subcortical white matter of early postnatal Cetartiodactyla (Tursiops truncatus, Stenella coeruloalba and Ovis aries). Brain Struct. Funct. *223*, 3613–3632.

Lazarini, F., and Lledo, P.M. (2011). Is adult neurogenesis essential for olfaction? Trends Neurosci. *34*, 20–30.

Le Magueresse, C., Alfonso, J., Bark, C., Eliava, M., Khrulev, S., and Monyer, H. (2012). Subventricular zone-derived neuroblasts use vasculature as a scaffold to migrate radially to the cortex in neonatal mice. Cereb. Cortex *22*, 2285–2296.

Leuba, G., and Saini, K. (1997). Colocalization of parvalbumin, calretinin and calbindin D-28k in human cortical and subcortical visual structures. J. Chem. Neuroanat. *13*, 41–52.

Lois, C., and Alvarez-Buylla, A. (1994). Long-distance neuronal migration in the adult mammalian brain. Science *264*, 1145–1148.

Lois, C., García-Verdugo, J.M., and Alvarez-Buylla, A. (1996). Chain migration of neuronal precursors. Science *271*, 978–981.

Low, V.F., Faull, R.L.M., Bennet, L., Gunn, A.J., and Curtis, M.A. (2013). Neurogenesis and progenitor cell distribution in the subgranular zone and subventricular zone of the adult sheep brain. Neuroscience *244*, 173–187.

Luskin, M.B. (1993). Restricted proliferation and migration of postnatally generated neurons derived from the forebrain subventricular zone. Neuron *11*, 173–189.

Luzzati, F., Peretto, P., Aimar, P., Ponti, G., Fasolo, A., and Bonfanti, L. (2003). Glia-independent chains of neuroblasts through the subcortical parenchyma of the adult rabbit brain. Proc. Natl. Acad. Sci. USA *100*, 13036–13041.

Morton, P.D., Korotcova, L., Lewis, B.K., Bhuvanendran, S., Ramachandra, S.D., Zurakowski, D., Zhang, J., Mori, S., Frank, J.A., Jonas, R.A., et al. (2017). Abnormal neurogenesis and cortical growth in congenital heart disease. Sci. Transl. Med. *9*, eaah7029.

Palazzo, O., La Rosa, C., Piumatti, M., and Bonfanti, L. (2018). Do large brains of long-living mammals prefer non-newly generated, immature neurons? Neural Regen. Res. *13*, 633–634.

Paredes, I., Himmels, P., and Ruiz de Almodóvar, C. (2018). Neurovascular communication during CNS development. Dev. Cell *45*, 10–32.

Paredes, M.F., James, D., Gil-Perotin, S., Kim, H., Cotter, J.A., Ng, C., Sandoval, K., Rowitch, D.H., Xu, D., McQuillen, P.S., et al. (2016a). Extensive migration of young neurons into the infant human frontal lobe. Science *354*, aaf7073.

Parnavelas, J.G., Alifragis, P., and Nadarajah, B. (2002). The origin and migration of cortical neurons. Prog. Brain Res. *136*, 73–80.

Parolisi, R., Cozzi, B., and Bonfanti, L. (2017). Non-neurogenic SVZ-like niche in dolphins, mammals devoid of olfaction. Brain Struct. Funct. *222*, 2625–2639.

Peretto, P., Giachino, C., Aimar, P., Fasolo, A., and Bonfanti, L. (2005). Chain formation and glial tube assembly in the shift from neonatal to adult subventricular zone of the rodent forebrain. J. Comp. Neurol. *487*, 407–427.

Piumatti, M., Palazzo, O., La Rosa, C., Crociara, P., Parolisi, R., Luzzati, F., Lévy, F., and Bonfanti, L. (2018). Non-newly generated, "immature" neurons in the sheep brain are not restricted to cerebral cortex. J. Neurosci. *38*, 826–842.

Ponti, G., Aimar, P., and Bonfanti, L. (2006). Cellular composition and cytoarchitecture of the rabbit subventricular zone and its extensions in the forebrain. J. Comp. Neurol. *498*, 491–507.

Raju, C.S., Spatazza, J., Stanco, A., Larimer, P., Sorrells, S.F., Kelley, K.W., Nicholas, C.R., Paredes, M.F., Lui, J.H., Hasenstaub, A.R., et al. (2018). Secretagogin is expressed by developing neocortical GABAergic neurons in humans but not mice and increases neurite arbor size and complexity. Cereb. Cortex *28*, 1946–1958.

Rutishauser, U. (1988). Specification of cerebral cortical areas. Nat. Rev. Neurosci. *241*, 170–176.

Saikali, S., Meurice, P., Sauleau, P., Eliat, P.A., Bellaud, P., Randuineau, G., Vérin, M., and Malbert, C.H. (2010). A three-dimensional digital segmented and deformable brain atlas of the domestic pig. J. Neurosci. Methods *192*, 102–109.

Sanai, N., Alvarez-Buylla, A., and Berger, M.S. (2005). Neural stem cells and the origin of gliomas. N. Engl. J. Med. *353*, 811–822.

Sanai, N., Nguyen, T., Ihrie, R.A., Mirzadeh, Z., Tsai, H.H., Wong, M., Gupta, N., Berger, M.S., Huang, E., Garcia-Verdugo, J.M., et al. (2011). Corridors of migrating neurons in the human brain and their decline during infancy. Nature *478*, 382–386.

Sawamoto, K., Hirota, Y., Alfaro-Cervello, C., Soriano-Navarro, M., He, X., Hayakawa-Yano, Y., Yamada, M., Hikishima, K., Tabata, H., Iwanami, A., et al. (2011). Cellular composition and organization of the subventricular zone and rostral migratory stream in the adult and neonatal common marmoset brain. J. Comp. Neurol. *519*, 690–713.

Sorrells, S.F., Paredes, M.F., Velmeshev, D., Herranz-Pérez, V., Sandoval, K., Mayer, S., Chang, E.F., Insausti, R., Kriegstein, A.R., Rubenstein, J.L., and Alvarez-Buylla, A. (2019). Immature excitatory neurons develop during adolescence in the human amygdala. Nat. Commun. *10*, 2748–2815.

Snapyan, M., Lemasson, M., Brill, M.S., Blais, M., Massouh, M., Ninkovic, J., Gravel, C., Berthod, F., Götz, M., Barker, P.A., et al. (2009). Vasculature guides migrating neuronal precursors in the adult mammalian forebrain via brain-derived neurotrophic factor signaling. J. Neurosci. *29*, 4172–4188.

Stepien, B.K., Vaid, S., and Huttner, W.B. (2021). Length of the neurogenic period-a key determinant for the generation of upper-layer neurons during neocortex development and evolution. Front Cell Dev. Biol. *9*, 676911.

Tata, M., and Ruhrberg, C. (2018). Cross-talk between blood vessels and neural progenitors in the developing brain. Neuronal Signal. *2*, NS20170139.

Taupin, P. (2007). BrdU immunohistochemistry for studying adult neurogenesis: paradigms, pitfalls, limitations, and validation. Brain Res. Rev. *53*, 198–214.

Walton, R.M. (2012). Postnatal neurogenesis: of mice, men, and macaques. Vet. Pathol. *49*, 155–165.

Wang, C., Liu, F., Liu, Y.Y., Zhao, C.H., You, Y., Wang, L., Zhang, J., Wei, B., Ma, T., Zhang, Q., and Yang, Z. (2011). Identification and characterization of neuroblasts in the subventricular zone and rostral migratory stream of the adult human brain. Cell Res. *21*, 1534–1550.

Yan, Y.H., Van Brederode, J.F., and Hendrickson, A.E. (1995). Transient co-localization of calretinin, parvalbumin, and calbindin-D28K in developing visual cortex of monkey. J. Neurocytol. *24*, 825–837.

Zhao, X., Wang, Y., Wait, E., Mankowski, W., Bjornsson, C.S., Cohen, A.R., Zuloaga, K.L., and Temple, S. (2021). 3D image analysis of the complete ventricular-subventricular zone stem cell niche reveals significant vasculature changes and progenitor deficits in males versus females with aging. Stem Cell Rep. *16*, 836–850.